Proceedings of the 6th World Congress on Mechanical, Chemical, and Material Engineering (MCM'20)
~~Prague, Czech Republic~~ Virtual Conference – August, 2020
Paper No. HTFF 181
DOI: 10.11159/htff20.181

An Approach to Modelling the Manufacturing Process of Thermoset Composite Reinforced with 3D Woven

Mikhail Kiauka, Olga Pudeleva, Vladimir Sergeev, Aleksandr Tamm, Alexey Borovkov
Peter the Great St. Petersburg Polytechnic University
Polytechnicheskaya, 29, St. Petersburg, Russia
kiauka_myu@spbstu.ru; pudeleva_oa@spbstu.ru; sergeev_vn@spbstu.ru; tamm@spbstu.ru; borovkov@spbstu.ru

Abstract **-** This paper proposes the general approach to modelling the manufacturing process of thermoset composite reinforced with 3D woven based on the digital twin concept. The focus is on the methodology for determining the permeability of a dry 3D woven. Simulation results in ANSYS CFX are presented. Also, a curing simulation technique in ABAQUS with user subroutines for a thermosetting composite is described. The results of curing simulation for the Kamal-Sourour model are presented in more detail and the prediction of shape distortion for a composite U-shaped part as a result of chemical shrinkage and thermal expansion is performed.

Keywords**:** Thermoset composite, 3D woven composites, Permeability, Transient heat transfer, Curing, Cure kinetics, Composite manufacturing, CFD, FEM

1. Introduction

Polymer composite materials are widely used in aerospace, automotive, energy and other fields. Recently, there has been a significant increase in the research and development of composite materials with the 3D woven preforms, in particular, to develop Gas Turbine Engine fan blades and housings (LEAP, GE9X engine blades) [1]. The manufacturing method of such parts is Liquid Composite Moulding (LCM). LCM comprises all the composite manufacturing methods, where the liquid state matrix material is forced into the dry preformed reinforcing material. A feature of structures made of composite materials is that the material and the part are formed simultaneously. In the manufacturing process various defects may occur: dry zones after impregnation, porosity; excessive residual stresses, which can induce destruction of the part even before the start of operation; unplanned the shape distortion. Such defects decrease the mechanical properties of the composite material, and distortion shape complicates assembly. Therefore, the implementation of virtual tests and the technology development based on them are an important task.

Manufacturing modelling of composite materials requires complex interdisciplinary researches, which includes modelling of hydrodynamics, deformable porous media, transient heat transfer, chemical kinetics, and mechanical behavior.

In particular, permeability characteristics of a dry preform (reinforcement) are required to perform impregnation modelling of the part. Curing simulation allows to determine the temperature and the degree of cure at each point of the part and to perform the following prediction of shape distortion.

E.B. Belov and S.V. Lomov choose the lattice Boltzmann method (LBM) for the numerical analysis of flow through a reinforcement using the software program written in C++ language [2]. LBM is used to simultaneously solve Navier–Stokes equations for the flow between yarns. The intra-yarn flow is accounted by solving the Brinkman equations. Developing this study B. Verleye and R. Croce present an approach to determine the velocity and pressure fields based on a finite difference discretization of the Stokes equations for inter-yarn flow [3], [4]. The advantages of this approach compared to modelling in commercial CFD software are quick calculation times, using of a voxel mesh, and correct intra-yarn flow accounting. But authors noted that there is a restriction on grid size and the use of physical models. Using this approach in [5] Elinor E. Swery performed permeability calculating for different 2D textiles. Numerical results without intra-yarn flow show good agreement with direct modelling in ANSYS CFX.

A. Endruweit and A.C. Long modeled the permeability of 3D woven carbon fiber fabrics based on geometrical parameters describing the textile architectures with using analytical model. [6]. A. M. Ali presented numerical computation

of through thickness permeability of two types of 3D woven fabrics by insitu compaction characterization using micro X-ray computed tomography [7].

C.C. Wong introduced inhomogeneities into the textile structure by randomly moving the tow paths and studied influence on the permeability for non-crimp fabric and plain weave models [8]. Long Li showed that the change of the fiber orientation and fiber volume fraction leads to the variety of permeability and, as a consequence, to the resin-rich areas in the composite and mechanical properties decreasing [9].

Numerical implementation of the model for prediction of the degree of cure, the associated heat and temperature increase of undiluted polymer resin is presented in [10]. J. Zhang, Y. C. Xu and P. Huang studied the influence of temperature cure cycle have on the temperature and degree of cure gradient [11]. In [12], [13] numerical discretization methods of the kinetics equations for adhesives are described. J. Magnus Svanberg and J. Anders Holmberg an approach for prediction of shape distortion for different constitutive models is presented [14]. M.V. Kozlov used the constitutive relations of CHILE (cure hardening instantaneously linear elastic) and Svanberg models modeled the influence of tool on the shape distortion [15].

There are many methods and some software for 2D textile composite manufacturing modelling. However, there is dearth of similar engineering methods and software for 3D textile composites.

The overall goal of our work is development of modelling approach for manufacturing process of composite materials with 3D woven preforms and a thermosetting matrix. It includes integrated techniques and algorithms with wide possibilities for automation and solving optimization problems. Now we propose to use a complex of CAE solutions, including commercial packages ANSYS CFX, ABAQUS and proprietary FORTRAN and Python codes.

In this paper a general modelling strategy and in more detail results of the woven preform permeability determination and composite curing simulation are presented.

2. General approach description

In our approach the manufacturing modelling of 3D woven composites includes the following main steps:

1) Creating of geometrical and finite element models of unit cell (UC) for a dry undeformed 3D woven.

2) Determination of the effective elastic properties of UC for a dry undeformed 3D woven.

3) Draping and compaction simulation of textile on a tool surface with using effective properties from step 2.

4) Dividing the textile into the finite number of regions where shear strain obtained in step 3 belongs to given range.

5) Shear strain averaging for regions obtained in step 4.

6) Application of average shear loading obtained in step 5 to the dry undeformed UC.

7) Determination of the permeability tensor components for deformed UC from step 6.

8) Modelling of textile preform impregnation for part with different permeability regions.

9) Homogenization and effective property's determination of the composite material for the rubbery and glassy matrix state for deformed UC obtained in step 6.

10) Transient heat transfer and cure kinetics modelling for part using effective elastic properties from step 9.

11) Residual stresses and strain determination for part, prediction of part shape distortion.

3. The permeability calculation

The influence of the internal geometry of the reinforcing preform at several length scales in the implicit form is taken into account by the components of the tensor $\boldsymbol{K}$, which, as a rule, are determined experimentally. To reduce the volume of time-consuming expensive tests, the role of numerical prediction of permeability increases.

Resin impregnation during vacuum infusion is a filtration of a fluid through a porous medium, which is described by Darcy's law:

$$\vec{u} = -\frac{1}{\mu}\boldsymbol{K} \cdot \nabla P \tag{1}$$

where $\vec{u}$ – flow velocity, μ – dynamic viscosity of resin, P – pressure, $\boldsymbol{K}$ – permeability tensor of porous medium. In some cases, it is possible to assume that $\boldsymbol{K}$ is a diagonal tensor.

A generalization of Darcy's law for different Reynolds numbers is the Forchheimer equation. In ANSYS CFX for Directional Loss Model, it is implemented as follows [16]:

$$\frac{dP}{dx} = -\frac{\mu}{K_{perm(x)}} u_x - K_{loss(x)} \frac{\rho}{2} |u| u_x \tag{2}$$

where: K_{perm} – permeability in x direction, m^2; K_{loss} – quadratic loss coefficients in x direction, 1/m; u – flow velocity in x direction, m/s; μ – gas dynamic viscosity, Pa·s; ρ – density of resin, kg/m^3.

The linear component of Eq. (2) represents viscous losses and the quadratic term represents inertial losses. There is a critical value of the Reynolds number depending on the geometric characteristics of the porous medium. At low speeds, the inertial losses can be neglected and the equation will comply with Darcy's law. At high speeds, inertial losses will prevail. In this study, it is assumed that the inertial losses are negligible because the Reynolds number is less than 1.

Thus, from equation (2) neglecting inertial losses permeability coefficient is defined as:

$$K_{perm} = \frac{G\mu L}{A\rho\Delta P} \tag{3}$$

where: G – resin mass flow rate, kg/m^3; L - the length over which the pressure drop is taking place, m; A – the cross-sectional area to flow, m^2; ΔP – pressure drop, Pa.

In case the model is limited to creeping, single-phase, isothermal, unidirectional saturated flow of a Newtonian fluid, the inter-yarn flow is described by the incompressible Navier-Stokes equations:

$$\begin{gathered} \frac{\delta\vec{u}}{\delta t} = -(\vec{u}\cdot\nabla)\vec{u} + \frac{1}{\rho}(\mu\Delta\vec{u} - \nabla P) \\ \nabla\cdot\vec{u} = 0 \end{gathered} \tag{4}$$

The first equation states the conservation of momentum (momentum equation), the second equation states conservation of mass (continuity equation).

Intra-yarn flow depends on the local permeability tensor of the tow K_{tow}, and is described by the Brinkman equations without neglecting the convection [2], [17]:

$$\begin{cases} \dfrac{\delta\vec{u}}{\delta t} = -(\vec{u}\cdot\nabla)\vec{u} + \dfrac{1}{\rho}(\mu\Delta\vec{u} - \mu\boldsymbol{K}_{tow}^{-1}\cdot\vec{u} - \nabla P) \\ \nabla\cdot\vec{u} = 0 \end{cases} \tag{5}$$

To determine the local permeability tensor K_{tow} along the fibers and in the transverse direction, the fibers were locally approximated as a regular cylinder array. According to formulas in [2] K_{tow} is 10^{-15} m^2. In [4] it is noted that for yarns K_{tow} is typically $10^{-10}…10^{-13}$ m^2.

Simulation neglecting intra-yarn flow and taking it into account has been performed. In this paper, we do not determine all the components of the tensor $\boldsymbol{K}$. The permeability value was determined by warp (K_{warp}), weft (K_{weft}) and through thickness (K_{tt}) directions of UC. Boundary condition as pressure gradient is defined. In each case, periodic boundary conditions are specified at another sides of UC. ANSYS CFX simulation result is mass flow. Permeability value

is defined with using Darcy's law from Eq. (3). In Fig.1 resin flow simulation results are shown for weft direction. Permeability prediction good correlation with literature data for 2D and 3D textiles has been showed (Table 1).

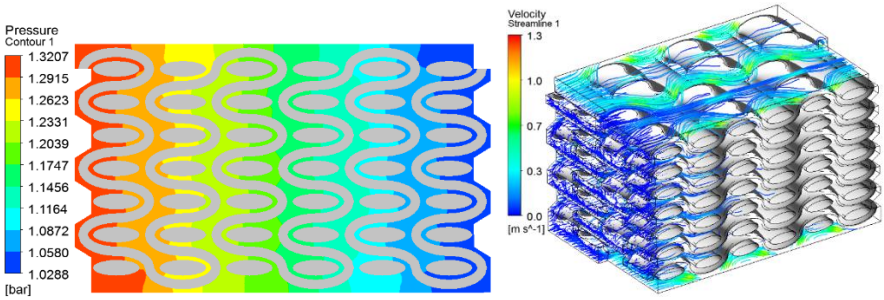

Fig. 1: Pressure field (left) and velocity streamlines (right) for inter-yarn flow in weft direction.

Table 1: Permeability coefficient calculation results.

Model	K_{warp}, m^2	K_{weft}, m^2	K_{tt}, m^2
Inter-yarn flow	$2{,}5\cdot10^{-9}$	$1{,}7\cdot10^{-9}$	$5{,}9\cdot10^{-10}$
Inter-yarn flow and intra-yarn flow	$3{,}43\cdot10^{-9}$	$2{,}1\cdot10^{-9}$	$7{,}1\cdot10^{-10}$
Literature data for 3D textile [18]	$3{,}5\cdot10^{-10}$	$4{,}5\cdot10^{-10}$	$5\cdot10^{-11}$
Literature data for different 2D textiles (numerical results) [5]	$2\cdot10^{-9}\div3{,}5\cdot10^{-11}$	$2\cdot10^{-9}\div3{,}5\cdot10^{-11}$	-

Comparison with [18], including the results of numerical and experimental studies, shows that the permeability coefficients obtained in our work are large. This is due to the "ideal" nature of the weave in the UC – the yarns do not touch each other and are located with a gap.

When taking into account intra-yarn flow, tow is represented by porous medium. In this case the total permeability of the reinforcing material is greater. It seems appropriate for a large volume fraction of fibers for UC, because otherwise $K_{tow} \ll K_{UC}$. Also for intra-yarn flow additional research of the fluid-porous interface is required because the impact of the transition region between fluid and porous regions on the interface stress balance is not well understood [19].

4. Cure kinetics simulation

Cure model has been implemented in ABAQUS with a user subroutine HETVAL. In virtual tests a cure cycle in the furnace/autoclave and typical heat transfer coefficients on the part and tool surface is specified. The temperature distribution is defined by the heat equation and Fourier's heat law:

$$\rho \frac{\delta(C_p T)}{\delta t} = k_{ij} \nabla^2 T + q \tag{6}$$

where ρ is density, C_p is specific heat capacity, T is temperature, k_{ij} ($i,j = x, y, z$) is the heat conductivity tensor components, ∇ denotes the Laplace operator, q is internal heat generation rate in a material as a result of an exothermic reaction.

Internal heat generation is defined as:

$$q = \rho_m H_T (1 - V_f) \frac{d\alpha}{dt} \tag{7}$$

where ρ_m; H_T; V_f and $d\alpha/dt$ is density of the matrix, total heat released by the matrix during the curing reaction (energy per unit mass), fiber volume fraction, respectively, the chemical reaction rate.

In further development, it is supposed to clarify the actual distribution and values of the heat transfer coefficients on the part and tool surface by airflow simulation using ANSYS CFX.

The cure degree, cure rate and temperature at each integration point during a cure cycle are defined at each time step. For this the cure kinetics equation was integrated by the improved Euler's method. The thermal conductivity tensor components of the composite, specific heat, density and viscosity of the resin were defined by the functions of the process temperature and degree of cure.

During cure three states of the matrix are successively replaced – liquid, rubbery and glassy. The dependence of the glass transition temperature T_g on the degree of cure α was defined using the Di Benedetto equation:

$$\frac{T_g - T_{g0}}{T_{g\infty} - T_{g0}} = \frac{\lambda\alpha}{1 - (1-\lambda)\alpha} \tag{8}$$

where T_{g0} and $T_{g\infty}$ are the glass transition temperature of the uncured (α = 0), respectively, fully cured system (α = 1); λ is a material constant.

In our algorithm depending on the thermoset polymer type, the following cure reaction formulations are implemented: n^{th} order, Prout-Tompkins autocatalytic and Kamal-Sourour (Eq. (9) - (11), respectively) [20]. Which model to use can be determined by examining heat flow measurements (e.g. from differential scanning calorimetry – DSC).

$$\frac{d\alpha}{dt} = K(T)(1-\alpha)^n \tag{9}$$

$$\frac{d\alpha}{dt} = K(T)\alpha^m(1-\alpha)^n \tag{10}$$

$$\frac{d\alpha}{dt} = (K_1 + K_2\alpha^m)(1-\alpha)^n \tag{11}$$

$$K(T) = A \cdot \exp\left[\frac{-E_a}{RT}\right] \tag{12}$$

where $K(T)$ – an Arrhenius-type relation for the reaction temperature dependency; A is the pre-exponential factor; m, n – model constants; E_a is the apparent activation energy; R is the universal gas constant; T is the temperature.

To check the model and FORTRAN code a test simulation for the U-shaped (60×40×20 mm) part was performed. Temperature cure cycle and boundary conditions shown in the Fig.2 and Fig.3, respectively. Boundary conditions include constraints, heat transfer coefficient α, heat flux from tool q_t. Constraints of the model simulates the location of the part on a tool (iso-static mounting).

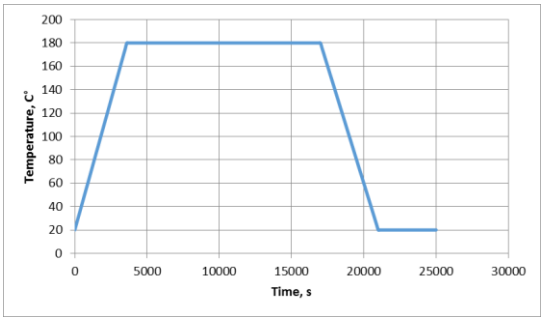

Fig. 2: Temperature cure cycle.

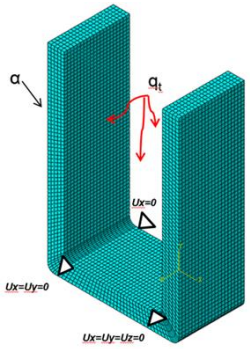

Fig. 3: Boundary conditions.

Results of cure simulation for Kamal-Sourour model presented in Fig. 4-7. Residual strains are induced by chemical shrinkage during cure and thermal expansion during cooling. The mechanical behavior model of the part is not described in detail in this paper, but the results presented in the Fig. 6-7 include thermal and mechanical effects. The qualitative picture of the deformation corresponds to the experimentally observed decrease in the angle of L-shaped and U-shaped parts. Angular deviation is 1,8 degrees.

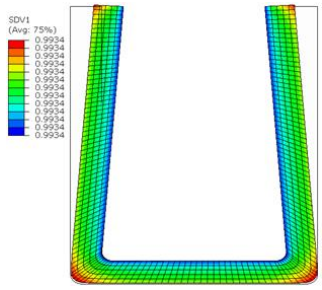

Fig. 4: Cure degree after 17000 s.

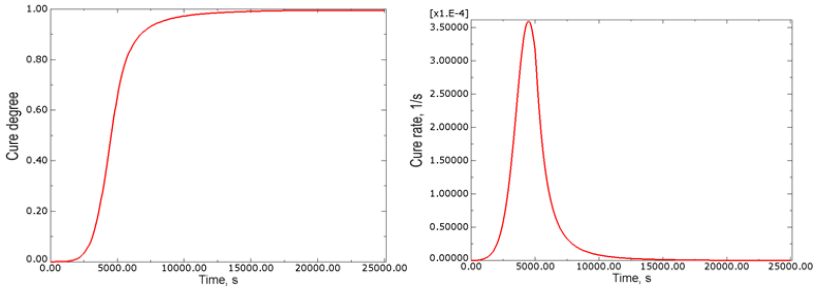

Fig. 5: Cure degree and cure rate at the laminate centre point.

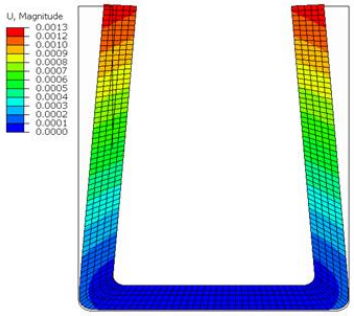

Fig. 6: Displacement (m) after 17000 s (the main contribution to shape distortion is chemical shrinkage).

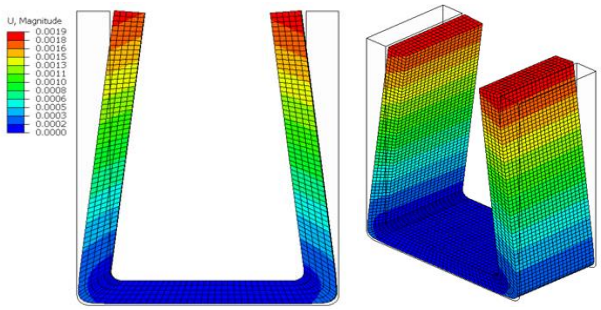

Fig. 7: Displacement (m) after 25000 s (the main contribution to shape distortion is thermal expansion).

4. Conclusion

General approach proposed in this paper permits to modelling the manufacturing process of thermoset composite reinforced with 3D woven. This approach can be used for both 3D textile and 2D textile composites.

In further development the components of the permeability tensor will be determined after compaction and drapery of the textile. It will be study in which cases the flow inside the yarn can be neglected. It is also necessary to study the effect of periodicity cell size on permeability.

When modelling curing in the future, a tool will be added to the finite element model to more accurately take into account the effect of temperature expansion of the tool on shape distortion, mechanical and thermal contacts between the part and tool.

References

[1] A. R. Wadia, “Technologies for the next engine generation,” *29th Congr. Int. Counc. Aeronaut. Sci. ICAS 2014*, 2014.

[2] E. B. Belov, S.V. Lomov, Ignaas Verpoest, T. Peters, D. Roose, R.S. Parnas, K. Hoes, H. Sol., “Modelling of permeability of textile reinforcements: Lattice Boltzmann method,” *Compos. Sci. Technol.*, vol. 64, no. 7–8, pp. 1069–1080, 2004.

[3] B. Verleye, M. Klitz, and R. Croce, “Predicting the permeability of textile reinforcements via a hybrid navierstokes/brinkman solver,” *... Conf. Flow ...*, no. July, pp. 65–72, 2006.

[4] B. Verleye, R. Croce, M. Griebel, M. Klitz, S.V. Lomov, G. Morren, H. Sol, I. Verpoest, D. Roose, "Permeability of Textile Reinforcements: Simulation; Influence of Shear, Nesting and Boundary Conditions; Validation," *9th Int. Conf. Flow Process. Compos. Mater.*, vol. 9, no. July, pp. 1–29, 2008.
[5] E. E. Swery, R. Meier, S. V. Lomov, K. Drechsler, and P. Kelly, "Predicting permeability based on flow simulations and textile modelling techniques: Comparison with experimental values and verification of FlowTex solver using Ansys CFX," *J. Compos. Mater.*, vol. 50, no. 5, pp. 601–615, 2016, doi: 10.1177/0021998315579927.
[6] A. Endruweit and A. C. Long, "Analytical permeability modelling for 3D woven reinforcements," *ICCM Int. Conf. Compos. Mater.*, 2009.
[7] A. M. Ali, K. A. Khan, and R. Umer, "Through thickness permeability and compaction characterization of 3D preforms using in-situ μxCT," *2018 Adv. Sci. Eng. Technol. Int. Conf. ASET 2018*, pp. 1–6, 2018.
[8] C. C. Wong, A. C. Long, and C. D. Rudd, "MODELLING THE EFFECTS OF FABRIC STRUCTURE ON THE VARIABILITY OF PERMEABILITY," no. July, pp. 47–54, 2006.
[9] L. Li, Y. Zhao, X. Zhao, S. Liu, G. Liu, and J. Bao, "The effect of preforming quality on the permeability of non-crimp fabrics and the mechanical properties of their composites," *ICCM Int. Conf. Compos. Mater.*, vol. 2015-July, no. July, pp. 19–24, 2015.
[10] S. Heinze and A. T. Echtermeyer, "A practical approach for data gathering for polymer cure simulations," *Appl. Sci.*, vol. 8, no. 11, pp. 1–31, 2018.
[11] J. Zhang, Y. C. Xu, and P. Huang, "Effect of cure cycle on curing process and hardness for epoxy resin," *Express Polym. Lett.*, vol. 3, no. 9, pp. 534–541, 2009.
[12] Z. Qin, S. Bin, W. Simin, X. Ling, and L. Sheng, "Cure kinetics analysis and simulation of silicone adhesives," *2009 Int. Conf. Electron. Packag. Technol. High Density Packag. ICEPT-HDP 2009*, no. August, pp. 691–694, 2009.
[13] A. G. Cassano, S. E. Stapleton, C. J. Hansen, and M. Maiaru, "Prediction of Cure Overheating in Thick Adhesive Bondlines for Wind Energy Applications," pp. 1–10.
[14] J. M. Svanberg and J. A. Holmberg, "Prediction of shape distortions Part I. FE-implementation of a path dependent constitutive model," *Compos. Part A Appl. Sci. Manuf.*, vol. 35, no. 6, pp. 711–721, 2004.
[15] M. V. Kozlov, S. V. Sheshenin, I. V. Makarenko, and D. A. Belov, "Modeling the influence of tooling on the final shape of polymer composite parts," *Comput. Contin. Mech.*, vol. 9, no. 2, pp. 145–161, 2016.
[16] *ANSYS CFX-Solver Theory Guide*. 2011.
[17] H. Verschoor, "Experimental data on the viscous force exerted by a flowing fluid on a dense swarm of particles," *Appl. Sci. Res.*, vol. 2, no. 1, pp. 155–161, 1951.
[18] X. S. Zeng, a C. Long, F. Gommer, A. Endruweit, and M. Clifford, "3D Carbon Reinforcements," in *18th International Conference on Composite Materials*.
[19] C. Degroot, "Stress Closure at the Interface Between Fluid and Porous Regions in ANSYS CFX Stress Closure at the Interface Between Fluid and Porous Regions in ANSYS CFX," no. May 2013, 2018.
[20] Menczel, J. D., and R. B. Prime. Thermal Analysis of Polymers, Fundamentals and Applications. 1st ed. New York: Wiley, 2009. Print.